

Spectral characteristics for a spherically confined $-a/r + br^2$ potential

Richard L. Hall ¹, Nasser Saad ², and K. D. Sen ³

¹ *Department of Mathematics and Statistics, Concordia University,
1455 de Maisonneuve Boulevard West, Montréal, Québec, Canada H3G 1M8**

² *Department of Mathematics and Statistics, University of Prince Edward Island,
550 University Avenue, Charlottetown, PEI, Canada C1A 4P3.† and*

³ *School of Chemistry, University of Hyderabad 500046, India.‡*

We consider the analytical properties of the eigenspectrum generated by a class of central potentials given by $V(r) = -a/r + br^2$, $b > 0$. In particular, scaling, monotonicity, and energy bounds are discussed. The potential $V(r)$ is considered both in all space, and under the condition of spherical confinement inside an impenetrable spherical boundary of radius R . With the aid of the asymptotic iteration method, several exact analytic results are obtained which exhibit the parametric dependence of energy on a , b , and R , under certain constraints. More general spectral characteristics are identified by use of a combination of analytical properties and accurate numerical calculations of the energies, obtained by both the generalized pseudo-spectral method, and the asymptotic iteration method. The experimental significance of the results for both the free and confined potential $V(r)$ cases are discussed.

PACS numbers: 31.15.-p 31.10.+z 36.10.Ee 36.20.Kd 03.65.Ge.

Keywords: oscillator confinement, confined hydrogen atom, discrete spectrum, asymptotic iteration method, generalized pseudo-spectral method

I. INTRODUCTION

The model for a hydrogen atom, HA, confined in an impenetrable sphere of finite radius R was originally introduced [1] to simulate the effect of high pressure on atomic static dipole polarizability. Sommerfeld and Welker [2] formulated the wave function solutions for this potential in terms of confluent hypergeometric functions, and underlined the application of this model for the prediction of the line spectrum originating from atomic hydrogen in the outer atmosphere. An algorithm for obtaining nearly exact energy calculations for a spherically confined hydrogen atom has been published [3]. On the other hand, regular soft confinement of the Coulombic systems has been developed by superimposing Debye screening [4]. Such a confining potential has been successful in explaining [5, 6] the shift in frequency of the x-ray spectral lines emitted by laser-imploded plasmas in the limit of high plasma density, whereby the effective potential assumes the form given by the Coulomb plus oscillator potential. The harmonic potential can be considered here as giving rise to the confinement of the Coulomb system with soft boundary walls. A variety of other model potentials leading to the confinement of electrons in atoms and molecules have been proposed, in order to explain the behavior of the novel artificial nanostructures, such as quantum wires and quantum dots, atoms and molecules embedded inside fullerenes, zeolites and liquid helium droplets, and, in addition, to simulate the interior of a giant planet. A comprehensive review covering of the development and applications of confining model potentials has been recently published [7, 8]. Under the confinement effect of an impenetrable spherical cavity of radius R , the hydrogen atom and the isotropic harmonic oscillator, IHO, potentials have been studied, independently, and their spectral characteristics have been analyzed [9, 10] in terms of useful quasi exact results. In the following text, we shall denote the spherically confined hydrogen atom as SCHA and the spherically confined isotropic harmonic oscillator as SCIHO: in both cases, the eigenstates are labelled as (ν, ℓ) , $\nu = 1, 2, 3, \dots$, $\ell = 0, 1, 2, \dots$, in terms of which the number of radial nodes for a given ℓ becomes $\nu - \ell - 1$.

For the *free* Coulomb plus oscillator potential, a few exploratory calculations have been reported earlier [11–14]. In view of the importance of the conjoined Coulomb and harmonic oscillator potential, it useful to study the general

*Electronic address: rhall@mathstat.concordia.ca

†Electronic address: nsaad@upei.ca

‡Electronic address: sensc@uohyd.ernet.in

behavior of this potential under the confinement due to an impenetrable spherical cavity, as a function of the radius R , where the free state is represented by $R \rightarrow \infty$. In this paper we consider a general spherically symmetric model of atomic system confined by (i) the presence of a harmonic-oscillator potential term and in a representative set of cases also (ii) containment inside an impenetrable spherical box of radius R . In atomic units $\hbar = m = e = 1$ the Hamiltonian for the model system is given by

$$H = -\frac{1}{2}\Delta + V(r), \quad V(r) = -\frac{a}{r} + br^2, \quad (1)$$

where a and b are coupling parameters. We shall always assume that $b > 0$ and for the most part, we shall assume that the Coulomb term is also attractive, $a > 0$; we shall also consider the repulsive case $a < 0$, in which H becomes a model, for example, for a system composed of a pair of confined electrons.

We shall now present a brief review of the known results defining the spectral characteristics of the two confined systems SCHA and SCIHO. It is well known that the so called *accidental degeneracy* of free HA is removed in the SCHA. As $R \rightarrow 0$, the energy levels $E(\nu, \ell)$ increase in magnitude such that the higher ℓ states get relatively less destabilized. There exists a critical value of R above which $E(\nu, \ell) > 0$. Further, two additional kinds of degeneracies arise [9]. They result from the specific choice of the radius of confinement R , chosen exactly at the radial nodes corresponding to the free HA wave functions. In the *incidental degeneracy* case, a given confined $(\nu = \ell + 1, \ell)$ state becomes iso-energetic with $(\nu = \ell + 2, \ell)$ state of the *free* HA with energy $-1/\{2(\ell + 2)^2\}$ a.u., at the same R . In the *simultaneous degeneracy* case, on the other hand, a certain pair of confined states at the common radius of confinement R that is prescribed in terms of the location of the radial node in a specific free state of HA, become iso-energetic. For example, for all $\nu \geq \ell + 2$, each (ν, ℓ) SCHA state is degenerate with $(\nu + 1, \ell + 2)$ state, when both of them are confined at $R = (\ell + 1)(\ell + 2)$, which defines the radial node in the free $(\ell + 2, \ell)$ state. Both these degeneracies have been shown [9] to result from the Gauss relationship applied at a unique R by the confluent hypergeometric functions that describe the general solutions of the SCHA problem.

We note that free IHO energy levels show the well-known “ $(2\nu + \ell)$ ” degeneracy with the equidistant eigenvalues given by $(2\nu + \ell - \frac{1}{2})\hbar\omega$, $\nu = 1, 2, 3, \dots$, for a given ℓ . Such a degeneracy is removed under the confined conditions. As $E(\nu, \ell) > 0$ at all R , the critical radius is absent. The *incidental degeneracy* observed in the case of SCIHO is qualitatively similar to that of the SCHA. However, the behavior of the two confined states at a common radius of confinement is found to be different [10, 15]. In particular, for the SCIHO the pairs of the confined states defined by $(\nu = \ell + 1, \ell)$ and $(\nu = \ell + 2, \ell + 2)$ at the common $R = \sqrt{(2\ell + 3)}/2$ a.u., display for all ν , a constant energy separation of *exactly* 2 harmonic-oscillator units, $2\hbar\omega$, with the state of higher ℓ corresponding to lower energy. The choice of R is qualitatively similar to that in the case of SCHA, namely, it is the location of the radial node in the $(\nu = \ell + 1, \ell)$ state which is the first excited state corresponding to a given ℓ for the free IHO. It is interesting to note that the two confined states at the common R with $\Delta\ell = 2$, considered above, contain different numbers of radial nodes.

With this background, we shall now consider the spherically confined potential defined in Eq.(1). The paper is organized as follows. In section 2, the scaling properties and monotonicity of the eigenspectrum generated by the potential $V(r)$, as a function of the parameters of the potential, are derived. Analytic energy bounds, derived by the envelope method, are reported in section 3: these are found to be useful in guiding the search for very accurate values by numerical methods. In sections 4 and 5, we use the asymptotic iteration method (AIM) to study how the eigenvalues depend on the potential parameters $\{a, b, R\}$, respectively for the free system ($R = \infty$), and for finite R . In each of these sections, the results obtained are of two types: exact analytic results that are valid when certain parametric constraints are satisfied, and accurate numerical values for arbitrary sets of potential parameters. In section 6 we adjoin some more numerical data, obtained by the generalized pseudo-spectral (GPS) Legendre method, and present a detailed analysis of the spectral characteristics of the system and their experimental significance.

II. SCALING AND MONOTONICITY

Since the potential and the confining box are spherically symmetric, we may write the energy eigenfunctions in the form

$$\Psi(\mathbf{r}) = \frac{\psi(r)}{r} Y_\ell^m(\theta, \phi), \quad \psi(0) = 0, \quad (2)$$

where $\mathbf{r} \in \mathfrak{R}^3$ and $r = |\mathbf{r}|$. For finite box sizes R we also require $\psi(R) = 0$. In terms of the atomic units used, each discrete eigenvalue depends on three parameters. We shall express this by writing $E_{\nu\ell} = E(a, b, R)$. If we now

introduce a scale factor (dilation) $\sigma > 0$ into the terms of the Hamiltonian, so that $r \rightarrow \sigma r$, then, after multiplying the eigenequation $H\psi = E\psi$ through by σ^2 , we may derive the general scaling law

$$E(a, b, R) = \sigma^{-2} E(\sigma a, \sigma^4 b, R/\sigma), \quad \sigma > 0. \quad (3)$$

For example, the particular choices $\sigma = a^{-1}$, $\sigma = b^{-\frac{1}{4}}$, and $\sigma = R$, then yield, respectively, the special scaling laws

$$E(a, b, R) = a^2 E(1, ba^{-4}, aR) = b^{\frac{1}{2}} E(ab^{-\frac{1}{4}}, 1, b^{\frac{1}{4}} R) = R^{-2} E(aR, bR^4, 1). \quad (4)$$

Thus it would be sufficient to consider just two spectral parameters.

The eigenvalues $E_{\nu, \ell} = E(a, b, R)$ are monotonic in each parameter. For a and b , this is a direct consequence of the monotonicity of the potential V in these parameters. Indeed, since $\partial V/\partial a = -1/r < 0$ and $\partial V/\partial b = r^2 > 0$, it follows that

$$\frac{\partial E(a, b, R)}{\partial a} < 0 \quad \text{and} \quad \frac{\partial E(a, b, R)}{\partial b} > 0. \quad (5)$$

The monotonicity with respect to the box size R may be proved by a variational argument. We shall show in section (III) that the Hamiltonian H is bounded below. The eigenvalues of H may therefore be characterized variationally. Let us consider two box sizes, $R_1 < R_2$ and an angular momentum subspace labelled by a fixed ℓ . We extend the domains of the wave functions in the finite-dimensional subspace spanned by the first N radial eigenfunctions for $R = R_1$ so that the new space W may be used to study the case $R = R_2$. We do this by defining the extended eigenfunctions so that $\psi_i(r) = 0$ for $R_1 \leq r \leq R_2$. We now look at H in W with box size R_2 . The minima of the energy matrix $[(\psi_i, H\psi_j)]$ are the exact eigenvalues for R_1 and, by the Rayleigh-Ritz principle, these values are one-by-one upper bounds to the eigenvalues for R_2 . Thus, by formal argument we deduce what is perhaps intuitively clear, that the eigenvalues increase as R is decreased, that is to say

$$\frac{\partial E(a, b, R)}{\partial R} < 0. \quad (6)$$

From a classical point of view, this Heisenberg-uncertainty effect is perhaps counter intuitive: if we try to squeeze the electron into the Coulomb well by reducing R , the reverse happens; eventually, the eigenvalues become positive and arbitrarily large, and less and less affected by the presence of the Coulomb singularity.

For some of our results we shall consider the system unconstrained by a spherical box, that is to say $R = \infty$. For these cases, we shall write $E_{\nu \ell} = E(a, b)$. If a very special box is now considered, whose size R coincides with any radial node of the $R = \infty$ problem, then the two problems share an eigenvalue exactly. This is an example of a very general relation which exists between constrained and unconstrained eigensystems, and, indeed, also between two constrained systems with different box sizes.

III. SOME ANALYTICAL ENERGY BOUNDS

The generalized Heisenberg uncertainty relation may be expressed [16, 17] as the operator inequality $-\Delta > 1/(4r^2)$. This allows us to construct the following lower energy bound

$$E > \mathcal{E} = \min_{0 < r \leq R} \left[\frac{1}{8r^2} - \frac{a}{r} + br^2 \right]. \quad (7)$$

Provided $b \geq 0$, this lower bound is finite for all a . It also obeys the same scaling and monotonicity laws as E itself. But the bound is weak. For potentials such as $V(r)$ that satisfy $\frac{d}{dr}(r^2 \frac{dV}{dr}) > 0$, Common has shown [18] for the ground state that $\langle -\Delta \rangle > \langle 1/(2r^2) \rangle$, but the resulting energy lower bound is still weak.

For the unconstrained case $R = \infty$, however, envelope methods [19–23, 25] allow one to construct analytical upper and lower energy bounds with general forms similar to (7). In this case we shall write $E_{\nu \ell} = E(a, b)$. Upper and lower bounds on the eigenvalues are based on the geometrical fact that $V(r)$ is at once a concave function $V(r) = g^{(1)}(r^2)$ of r^2 and a convex function $V(r) = g^{(2)}(-1/r)$ of $-1/r$. Thus tangents to the g functions are either shifted scaled oscillators above $V(r)$, or shifted scaled atoms below $V(r)$. The resulting energy-bound formulas are given by

$$\min_{r > 0} \left[\frac{1}{2r^2} - \frac{a}{P_1 r} + b(P_1 r)^2 \right] \leq E_{\nu \ell}(a, b) \leq \min_{r > 0} \left[\frac{1}{2r^2} - \frac{a}{P_2 r} + b(P_2 r)^2 \right], \quad (8)$$

where (Ref. [24] Eq.(4.4))

$$P_1 = \nu, \quad P_2 = 2\nu - (\ell + \frac{1}{2}). \quad (9)$$

We use the convention of atomic physics in which, even for non-Coulombic central potentials, a principal quantum number ν is used and defined by $\nu = n + \ell + 1$, where n is the number of nodes in the radial wave function. It is clear that the lower energy bound has the Coulombic degeneracies, and the upper bound those of the harmonic oscillator. These bounds are very helpful as a guide when we seek very accurate numerical estimates for these eigenvalues.

Another related estimate is given by the ‘sum approximation’ [23] which is more accurate than (8) and is known to be a lower energy bound for the bottom $E_{\ell+1\ell}$ of each angular-momentum sub space: in terms of the P ’s we have for these states, $P_2 = \nu + \frac{1}{2} = P_1 + \frac{1}{2}$. The estimate is given by

$$E_{\nu\ell}(a, b) \approx \mathcal{E}_{\nu\ell}(a, b) = \min_{r>0} \left[\frac{1}{2r^2} - \frac{a}{P_1 r} + b(P_2 r)^2 \right]. \quad (10)$$

This energy formula has the attractive spectral interpolation property that it is *exact* whenever a or b is zero. The energy bounds (8) and (10) obey the same scaling and monotonicity laws as those of $E_{\nu\ell}(a, b)$. Because of their simplicity they allow one to extract analytical properties of the eigenvalues. For example, we can estimate the critical oscillator coupling \hat{b} that will lead to vanishing energy $E = 0$. We may estimate \hat{b} by using (8) or (10). We differentiate with respect to r , and use the vanishing of this derivative and of E to obtain the following explicit formula for \hat{b}

$$\hat{b} \approx \left(\frac{27}{32} \right) \frac{a^4}{P_a^4 P_b^2}, \quad (11)$$

in which P_a and P_b are to be chosen. If $P_a = P_1$ and $P_b = P_2$, then from (10) we obtain a good general approximation for \hat{b} . We can also obtain bounds on \hat{b} . Since $E(a, b)$ is a monotone increasing function of b , we can state the nature of the bounds on \hat{b} given by formula (11): (i) if $P_a = P_b = P_1 = \nu$, the formula yields an upper bound; (ii) if $P_a = P_b = P_2 = 2\nu - (\ell + \frac{1}{2})$, then it is a lower bound; (iii) if $\nu = \ell + 1$ and $P_a = \nu$ and $P_b = \nu + \frac{1}{2}$, then the formula yields a lower bound. We shall state this last result explicitly: for the bottom of each angular-momentum subspace, where $\nu = \ell + 1$, the critical oscillator coupling \hat{b} yielding $E = 0$ is bounded by

$$\hat{b} \geq \left(\frac{27}{32} \right) \frac{a^4}{\nu^4 (\nu + \frac{1}{2})^2}. \quad (12)$$

IV. EXACT SOLUTIONS FOR THE POTENTIAL $V(r)$

The radial three-dimensional Schrödinger equation for the Coulomb plus harmonic-oscillator potential, expressed in atomic units, is given by

$$-\frac{1}{2} \frac{d^2 \psi(r)}{dr^2} + \left[\frac{l(l+1)}{2r^2} - \frac{a}{r} + br^2 \right] \psi(r) = E\psi(r), \quad 0 < r < \infty, \quad b > 0, \quad a \in \mathbb{R} \quad (13)$$

where $l(l+1)$ represents the eigenvalue of the square of the angular-momentum operator L^2 . Note that for $a = 0$, the potential $V(r) = -a/r + br^2$ corresponds to the pure harmonic oscillator potential, while for $a > 0$, it is a sum of two potentials, the attractive Coulomb term $-a/r$ plus the harmonic-oscillator potential br^2 . For $a < 0$, the potential $V(r)$ corresponds to the sum of two potentials, the repulsive Coulomb potential $|a|/r$ plus a harmonic-oscillator potential br^2 .

Since the harmonic oscillator potential dominates at large r , this suggests the following Ansatz for the wave function:

$$\psi(r) = r^{l+1} \exp(-\alpha r^2) f(r), \quad (14)$$

where α is a positive parameter to be determined. Substituting this wave function into Schrödinger’s equation (13), we obtain the following second-order differential equation for $f(r)$:

$$r f''(r) + (-4\alpha r^2 + 2l + 2) f'(r) + ((-2b + 4\alpha^2) r^3 + (-4\alpha l + 2E - 6\alpha) r + 2a) f(r) = 0, \quad (15)$$

For $n = 0$ we have, for the purely harmonic oscillator $a = 0$, the exact energy

$$E_{0l} = \left(l + \frac{3}{2}\right)\sqrt{2b} \quad (22)$$

which gives the ground-state $f_0(x) = 1$ in each subspace labelled by the angular momentum quantum number l .

For $n = 1$, the determinant $\Delta_2 = 0$ forces the potential parameters a and b to satisfy the equality

$$a^2 - \sqrt{2b}(l+1) = 0 \quad (23)$$

with a necessary condition for the eigenenergy

$$E_{1l} = \left(l + \frac{5}{2}\right)\sqrt{2b}. \quad (24)$$

The condition (23) gives two possibilities for the wavefunction solution. First, for $a = -\sqrt{\sqrt{2b}(l+1)}$, i.e. with repulsive Coulomb term, we have a ground-state (no-node) eigenfunction given by

$$\psi_0(r) = r^{l+1} \exp\left(-\sqrt{\frac{b}{2}} r^2\right) \left(1 + \sqrt{\frac{\sqrt{2b}}{l+1}} r\right), \quad (25)$$

while for $a = \sqrt{\sqrt{2b}(l+1)}$, i.e. an attractive Coulomb term, we have a first-excited state (one-node):

$$\psi_1(r) = r^{l+1} \exp\left(-\sqrt{\frac{b}{2}} r^2\right) \left(1 - \sqrt{\frac{\sqrt{2b}}{l+1}} r\right). \quad (26)$$

In table (I), we report the first few exact solutions along with the conditions on the potential parameters. Note, the subscripts on the polynomial solutions $f_i(r)$ refer to the possible number of nodes n in the wave function.

TABLE I: Conditions for Exact Solutions, here $E_{nl} = \left(n + l + \frac{3}{2}\right)\sqrt{2b}$

n	$f_n(r)$
0	$f_0(r) = 1$
$a = 0$	
1	$f_{\substack{a < 0, n=0 \\ a > 0, n=1}}(r) = 1 - \frac{a}{l+1} r$
$a^2 - \sqrt{2b}(l+1) = 0$	
2	$f_{\substack{a=0, n=0 \\ a < 0, n=0 \\ a > 0, n=2}}(r) = 1 - \frac{a}{l+1} r + \frac{\sqrt{2b}}{l+1} r^2$
$a(a^2 - \sqrt{2b}(5+4l)) = 0$	
3	$f_{\substack{a > 0, n=1,2 \\ a < 0, n=0,1}}(r) = 1 - \frac{a}{l+1} r + \frac{a^2 - 3\sqrt{2b}(l+1)}{(l+1)(2l+3)} r^2 - \frac{1}{3} \frac{a(a^2 - \sqrt{2b}(7l+9))}{(l+1)(l+2)(2l+3)} r^3$
$a^4 - 5\sqrt{2b}(3+2l)a^2 + 18b(2+l)(1+l) = 0$	

For arbitrary values of a and b that do not satisfy the conditions (20) and (21), we may use the asymptotic iteration method [27] that can be summarized by the following theorem (for details, see [27], section V Theorem 1, and [28], equations (2.13)-(2.14)):

Theorem 3: Given $\lambda_0 \equiv \lambda_0(x)$ and $s_0 \equiv s_0(x)$ in C^∞ , the differential equation

$$y'' = \lambda_0(x)y' + s_0(x)y \quad (27)$$

has a general solution

$$y = \exp\left(-\int^x \alpha(t) dt\right) \left[C_2 + C_1 \int^x \exp\left(\int^t (\lambda_0(\tau) + 2\alpha(\tau)) d\tau\right) dt \right] \quad (28)$$

if for some $n > 0$

$$\frac{s_n}{\lambda_n} = \frac{s_{n-1}}{\lambda_{n-1}} = \alpha(x), \quad \text{or} \quad \delta_n(x) = \lambda_n s_{n-1} - \lambda_{n-1} s_n = 0, \quad (29)$$

where, for $n \geq 1$,

$$\begin{aligned} \lambda_n &= \lambda'_{n-1} + s_{n-1} + \lambda_0 \lambda_n, \\ s_n &= s'_{n-1} + s_0 \lambda_n. \end{aligned} \quad (30)$$

Thus, for Eq.(16), with $\lambda_0(r)$ and $s_0(r)$ given by

$$\begin{cases} \lambda_0(r) = -\frac{1}{r} \left(-2r^2 \sqrt{2b} + 2(l+1) \right), \\ s_0(r) = -\frac{1}{r} \left[\left(2E - (2l+3)\sqrt{2b} \right) r + 2a \right], \end{cases} \quad (31)$$

the asymptotic iteration sequence $\lambda_n(x)$ and $s_n(x)$ can be calculated iteratively using (30). The energy eigenvalues $E \equiv E_{nl}$ of Eq.(16) can be obtained as roots of the termination condition (29). According to the asymptotic iteration method (AIM), in particular the study of Brodie *et al* [29], unless the differential equation is exactly solvable, the termination condition (29) produces for each iteration an expression that depends on both r and E (for given values of the parameters a , b and l). In such a case, one faces the problem of finding the best possible starting value $r = r_0$ that stabilizes the AIM process [29]. For our problem, we find that the starting value of $r_0 = 4$ is sufficient to utilize AIM without much worry about the best possible value of r_0 . For small values of a , where the wavefunction is spread out, we may increase $r_0 > 4$. In Table II, we report our numerical results, using AIM, for energies E_{nl} for the attractive ($a = 1$) and repulsive ($a = -1$) Coulomb term plus the harmonic-oscillator potential. The numerical computations in the present work were done using Maple version 13 running on an IBM architecture personal computer where we used a high-precision environment. In order to accelerate our computation we have written our own code for root-finding algorithm using a bisection method, instead of using the default procedure 'Solve' of *Maple 13*. The numerical results reported in Table II are accurate to the number of decimals reported. The subscript N refers to the number of iterations used by AIM.

TABLE II: Eigenvalues E_{nl} for $V(r) = -a/r + br^2$, where $b = 0.5$, $a = \pm 1$ and different n and l . The subscript N refer to the number of iteration used by AIM.

$b = 0.5$					
$a = 1$			$a = -1$		
n	l	E_{nl}	n	l	E_{nl}
1	0	2.500 000 000 000 000 000 $N=3, exact$	0	0	2.500 000 000 000 000 000 $N=3, exact$
	1	3.801 929 609 626 278 046 $N=80$		1	3.219 314 119 830 611 360 $N=74$
	2	4.930 673 420 047 524 772 $N=72$		2	4.087 227 795 734 562 981 $N=67$
	3	6.006 537 298 710 828 780 $N=65$		3	5.007 681 882 732 318 957 $N=61$
	4	7.058 140 776 824 529 475 $N=60$		4	5.953 327 675 284 371 524 $N=56$
0	0	0.179 668 484 653 553 873 $N=97$	1	0	4.380 233 836 413 610 273 $N=97$
	1	2.500 000 000 000 000 000 $N=3, Exact$		2	6.301 066 353 339 463 595 $N=67$
	2	4.631 952 408 873 053 214 $N=72$		3	8.243 517 978 923 477 298 $N=67$
	3	6.712 595 725 661 429 760 $N=70$		4	10.199 062 810 923 865 963 $N=65$
	4	8.769 519 600 328 899 714 $N=69$		5	12.163 259 523 048 320 928 $N=64$

V. EXACT SOLUTIONS FOR THE SPHERICALLY CONFINED $V(r)$

In this section, we consider the confined case of Coulomb and harmonic oscillator system as described by the radial Schrödinger equation (in atomic units)

$$-\frac{1}{2} \frac{d^2 \psi(r)}{dr^2} + \left[\frac{l(l+1)}{2r^2} - \frac{a}{r} + br^2 \right] \psi(r) = E\psi(r), \quad 0 < r < R, \quad b > 0. \quad (32)$$

where $l = 0, 1, \dots$ is the angular-momentum quantum number and $\psi(0) = \psi(R) = 0$. Here, again, the parameter a is allowed to in \mathbb{R} . Intuitively, we may assume the following ansatz for the wave function

$$\psi(r) = r^{l+1}(R-r) \exp(-\alpha r^2 - \beta r) f(r), \quad (33)$$

where α and β are parameters to be determine, and R is the radius of confinement. The $R-r$ factor ensures that the wave function will become zero at $r = R$. Direct substitution of Eq.(33) into Eq.(32) yields the following second-order linear differential equation for $f(r)$:

$$\begin{aligned} f''(r) = & -2 \left(\frac{l+1}{r} - \frac{1}{R-r} - 2\alpha r - \beta \right) f'(r) \\ & - \frac{1}{r(R-r)} \left[(2b - 4\alpha^2)r^4 + (4R\alpha^2 - 4\beta\alpha - 2Rb)r^3 + (4R\alpha\beta - 2E - \beta^2 + 4l\alpha + 10\alpha)r^2 \right. \\ & \left. + (R\beta^2 - 6R\alpha + 2RE - 4Rl\alpha + 2l\beta + 4\beta - 2a)r - 2(l+1) + 2Ra - 2R\beta(l+1) \right] f(r) \end{aligned} \quad (34)$$

Clearly, from this equation, we have $\alpha = \sqrt{b/2}$ and $\beta = 0$, which reveals the domination of the harmonic oscillator term even in the confined case. Consequently, for $f(r)$, we have

$$\begin{aligned} f''(r) = & -2 \left(\frac{l+1}{r} - \frac{1}{R-r} - \sqrt{2b} r \right) f'(r) \\ & - \frac{1}{r(R-r)} \left[(-2E + (2l+5)\sqrt{2b})r^2 + (-3R\sqrt{2b} + 2RE - 2Rl\sqrt{2b} - 2a)r - 2(l+1) + 2Ra \right] f(r) \end{aligned} \quad (35)$$

Although, equation (35) still does not lie within the framework of Theorem 1, we may make use of the following result ([26], Theorem 6)

Theorem 4. *A necessary condition for the second-order linear differential equation*

$$\left(\sum_{i=0}^{k+2} a_{k+2,i} x^{k+2-i} \right) y'' + \left(\sum_{i=0}^{k+1} a_{k+1,i} x^{k+1-i} \right) y' - \left(\sum_{i=0}^k \tau_{k,i} x^{k-i} \right) y = 0 \quad (36)$$

to have a polynomial solution of degree n is

$$\tau_{k,0} = n(n-1)a_{k+2,0} + na_{k+1,0}, \quad k = 0, 1, 2, \dots \quad (37)$$

Thus for Eq.(35), or, more explicitly, the differential equation

$$\begin{aligned} r(R-r)f''(r) + 2 \left((l+1)(R-r) - r - \sqrt{2b} r^2 R + \sqrt{2b} r^3 \right) f'(r) \\ + \left[(-2E + (2l+5)\sqrt{2b})r^2 + (-3R\sqrt{2b} + 2RE - 2Rl\sqrt{2b} - 2a)r + 2Ra - 2(l+1) \right] f(r) = 0 \end{aligned} \quad (38)$$

to have polynomial solutions of the form $f_n(r) = \sum_{k=0}^n a_k x^k$, it is necessary that

$$E_{nl} = (n+l + \frac{5}{2})\sqrt{2b}. \quad (39)$$

This is an important formula for E_{nl} that can facilitate greatly our computations based on AIM. We note, first, using Eq.(39) that Eq.(35) can be reduced to

$$\begin{aligned} f_n''(r) = & -2 \left(\frac{l+1}{r} - \frac{1}{R-r} - \sqrt{2b} r \right) f_n'(r) \\ & - \frac{1}{r(R-r)} \left[-2n\sqrt{2b} r^2 + (2R\sqrt{2b}(n+1) - 2a)r + 2Ra - 2(l+1) \right] f_n(r). \end{aligned} \quad (40)$$

- It is then clear from equation (40) that, for $n = 0$, we have

$$\begin{cases} E_{0l} = (l + \frac{5}{2})\sqrt{2b}, & f_0(r) = 1, \\ \psi_{0l}(r) = r^{l+1}(R - r) \exp(-\sqrt{\frac{b}{2}}r^2). \end{cases} \quad (41)$$

if the parameters a , b and the radius of confinement R are related by

$$aR = l + 1, \quad a^2 = (l + 1)\sqrt{2b}. \quad (42)$$

The wavefunction given by (41) represent the ground-state eigenfunction in each subspace labeled by the angular momentum quantum number l .

- For $n = 1$, we, easily, find that

$$\begin{cases} E_{1l} = (l + \frac{7}{2})\sqrt{2b}, & f_{0,1}(r) = 1 + \left(\frac{1}{R} - \frac{a}{l+1}\right)r, \\ \psi_{1l}(r) = r^{l+1}(R - r) \exp(-\sqrt{\frac{b}{2}}r^2) \left(1 + \left(\frac{1}{R} - \frac{a}{l+1}\right)r\right), \end{cases} \quad (43)$$

only if the parameters a , b and R are related by

$$\begin{cases} \sqrt{2b} = \frac{a}{R} - \frac{l+1}{R^2} \Rightarrow b = \frac{1}{2} \left(\frac{a}{R} - \frac{l+1}{R^2}\right)^2, \\ a = \frac{1}{R} \left(2l + \frac{5}{2} \pm \frac{1}{2}\sqrt{4l+5}\right). \end{cases} \quad (44)$$

Or, more explicitly, for a and b expressed in terms of the radius of confinement R , as

$$\begin{cases} a_{\pm} = \frac{1}{R} \left(2l + \frac{5}{2} \pm \frac{1}{2}\sqrt{4l+5}\right), \\ b_{\pm} = \frac{1}{8R^4} \left(\pm(3+2l) + \sqrt{4l+5}\right)^2, \end{cases} \quad \Rightarrow E = \frac{1}{2}(7+2l)\sqrt{2b}. \quad (45)$$

From (43), for $a > 0$, it is clear that either $a < (l+1)/R$ or $a > (l+1)/R$, since, for the case of $a = (l+1)/R$, we have $b = 0$, which is not acceptable from the structure of our wave function (33) where $b > 0$. We further note from (43) that for $r < R$ to have one node within $(0, R)$, it is necessary that $R > 2(l+1)/a > (l+1)/a$. For example, if $a = 1, l = 0$, then for a one-node state within $(0, R)$, it is required that $R > 2$. Thus, let $a = 1, l = 0, R = 5/2 + \sqrt{5}/2$, we have from (45), $b = 1/50$ and $E_{10} = 0.700\ 000\ 000\ 000\ 000$. Note further, if $a = 1, l = 0$ but $R = 5/2 - \sqrt{5}/2$, although $1/R < (l+1)/a$, still we do not have any node that lies within $(0, 5/2 - \sqrt{5}/2)$, since in this case $r = R = 5/2 - \sqrt{5}/2$. Thus we have, in this case, a node-less wave function $f_0(r)$ with $E_{00} = 0.699\ 999\ 999\ 995\ 412\ 275$. This explains the subscript $f_{0,1}$ in (43).

- Further, for $n = 2$, we can show that

$$\begin{cases} E_{2l} = \frac{1}{2}(9+2l)\sqrt{2b}, & f_{0,1,2}(r) = 1 + \left(\frac{1}{R} - \frac{a}{l+1}\right)r - \left(\frac{(3\sqrt{2b}(l+1)-a^2)R^2+(aR-l-1)(2l+3)}{R^2(l+1)(2l+3)}\right)r^2, \\ \psi_{2l}(r) = r^{l+1}(R - r) \exp(-\sqrt{\frac{b}{2}}r^2) \left(1 + \left(\frac{1}{R} - \frac{a}{l+1}\right)r - \left(\frac{(3\sqrt{2b}(l+1)-a^2)R^2+(aR-l-1)(2l+3)}{R^2(l+1)(2l+3)}\right)r^2\right), \end{cases} \quad (46)$$

only if a , b and R are related by the two-implicit expressions:

$$R^3 a^3 - 3R^2(l+2)a^2 - R(R^2\sqrt{2b}(7l+9) - 3(l+2)(2l+3))a - 3(l+2)(l+1)(2l+3 - 3R^2\sqrt{2b}) \quad (47)$$

and

$$R^2 a^3 - R(R^2\sqrt{2b} + 2l+3)a^2 + (l+1)(2l+3 - 3R^2\sqrt{2b})a + 6bR^3(l+1) = 0. \quad (48)$$

We now consider a few examples of these results:

- If $a = 1, l = 0$, then (47) and (48) yields $\sqrt{2b} = 0.76025880213480504582, R = 2.0843217092058454961$, and we have the following solution:

$$\begin{cases} E_{10} = 3.421\ 164\ 609\ 606\ 622\ 706\ 2, \\ \psi_{10}(r) = r(2.084\ 321\ 709\ 205\ 845\ 496\ 1 - r) \exp(-0.380\ 129\ 401\ 067\ 402\ 522\ 91\ r^2) \\ \quad \times (1 - 0.520\ 227\ 613\ 816\ 384\ 707\ 07\ r - 0.676\ 516\ 312\ 440\ 766\ 915\ 00\ r^2). \end{cases} \quad (49)$$

- If $\sqrt{2b} = 2, l = 0$, then (47) and (48) yields $a = -1.6219380762368883824, R = 1.0232416568868508038$ and we have the following solution:

$$\begin{cases} E_{00} = 9.000\ 000\ 000\ 000\ 000, \\ \psi_{00}(r) = r(1.023\ 241\ 656\ 886\ 850\ 803\ 8 - r) \exp(-r^2) \\ \quad \times (1 + 2.599\ 224\ 324\ 572\ 826\ 833\ 6\ r + 1.417\ 080\ 563\ 127\ 630\ 983\ 0\ r^2). \end{cases} \quad (50)$$

- For $n = 3$, we have

$$\begin{cases} E_{3l} = \frac{1}{2}(11 + 2l)\sqrt{2b} \\ f_2(r) = 1 + \left(\frac{1}{R} - \frac{a}{l+1}\right)r - \frac{R(4R\sqrt{2b}(l+1) - a(Ra - 3 - 2l)) - (2l+3)(l+1)}{R^2(2l+3)(l+1)}r^2 \\ \quad + \frac{1}{3} \frac{(-R^3a^3 + 3R^2(l+2)a^2 + R(R^2\sqrt{2b}(10l+13) - 3(l+2)(2l+3))a - 3(l+2)(l+1)(-2l+4R^2\sqrt{2b}-3))}{R^3(l+1)(l+2)(2l+3)}r^3 \end{cases} \quad (51)$$

where a, b and R are related by

$$R^3a^3 - R^2(R^2\sqrt{2b} + 3(l+2))a^2 - R(R^2\sqrt{2b}(10l+13) - 3(l+2)(2l+3))a \quad (52)$$

$$+ 2b(13 + 10l)R^4 + 12\sqrt{2b}(l+1)(l+2)R^2 - 3(2l+3)(l+2)(l+1) = 0 \quad (53)$$

and

$$\begin{aligned} R^4a^4 - 2R^3(2l+5)a^3 - R^2(R^2\sqrt{2b}(16l+25) - 6(2l+5)(l+2))a^2 + 2R(2l+5)(R^2\sqrt{2b}(10l+13) \\ - 3(l+2)(2l+3))a + 6(l+1)(l+2)((2l+5)(2l+3) + 4\sqrt{2b}R^2(R^2\sqrt{2b} - 5 - 2l)) = 0. \end{aligned} \quad (54)$$

Similar results can be obtain for higher n (the degree of the polynomial solutions). It is necessary to note that the conditions reported here are for the mixed potential $V(r) = -a/r + br^2$, where $a \neq 0, b \neq 0$ (neither coefficient is zero).

For the arbitrary values of a, b and R , not necessarily satisfying the above conditions, we still apply AIM directly to compute the eigenvalues. Similarly to the un-confined case, we start with

$$\begin{cases} \lambda_0(r) = -2 \left(\frac{l+1}{r} - \frac{1}{R-r} - \sqrt{2b} r \right), \\ s_0(r) = -\frac{1}{r(R-r)} \left[(-2E + (2l+5)\sqrt{2b})r^2 + (-3R\sqrt{2b} + 2RE - 2Rl\sqrt{2b} - 2a)r + 2Ra - 2(l+1) \right]. \end{cases} \quad (55)$$

The AIM sequence $\lambda_n(x)$ and $s_n(x)$ can be calculated iteratively using (30). The energy eigenvalues $E \equiv E_{nl}$ of Eq.(38) are obtained as roots of the termination condition (31). Since the differential equation (38) has two *regular* singular points at $r = 0$ and $r = R$, our initial value of r_0 can be chosen to be an arbitrary value in $(0, R)$. In table III, we reported the eigenvalues computed using AIM for a fixed radius of confinement $R = 1$ with $r_0 = 0.5$ as an initial value to seed the AIM process. In general, the computation of the eigenvalues are fast as illustrated by the small number of iteration N in Tables III, IV and V. The same procedure can be applied to compute the eigenvalues for arbitrary values of a, b and R . In Table IV we have fixed a, b and allowed R to vary, then we fixed b, R and allowed a to vary. In Table V, we fixed a, R and varied b . Our numerical results in these tables confirm our earlier monotonicity formulas reported in section II.

TABLE III: Eigenvalues E_{nl} for $V(r) = -a/r + br^2$, $r \in (0, R)$, where $b = 0.5$, $a = \pm 1$, $R = 1$ and different n and l . The subscript N refers to the number of iteration used by AIM.

$a = 1, b = 0.5, R = 1$											
n	l	E_{nl}				n	l	E_{nl}			
0	0	2.500 000 000 000 000 000 000 _{$N=3, Exact$}				0	0	2.500 000 000 000 000 000 000 _{$N=3, Exact$}			
1	1	8.404 448 391 842 929 575 _{$N=24$}				1	1	16.733 064 961 893 308 967 _{$N=25$}			
2	2	15.183 570 193 031 143 001 _{$N=23$}				2	2	41.029 002 263 262 675 364 _{$N=33$}			
3	3	23.137 256 709 545 767 885 _{$N=24$}				3	3	75.297 038 665 283 580 892 _{$N=40$}			
4	4	32.295 207 272 878 341 541 _{$N=27$}				4	4	119.493 804 921 354 632 859 _{$N=47$}			
$a = -1, b = 0.5, R = 1$											
n	l	E_{nl}				n	l	E_{nl}			
0	0	7.427 602 986 235 605 737 _{$N=26$}				0	0	7.427 602 986 235 605 737 _{$N=26$}			
1	1	12.118 629 877 542 593 085 _{$N=24$}				1	1	22.954 866 627 528 634 394 _{$N=27$}			
2	2	18.456 796 172 766 948 526 _{$N=23$}				2	2	48.054 781 032 847 609 425 _{$N=36$}			
3	3	26.173 002 039 626 403 748 _{$N=25$}				3	3	82.897 495 765 909 946 966 _{$N=41$}			
4	4	35.179 533 437 869 611 594 _{$N=28$}				4	4	127.540 759 830 804 826 131 _{$N=48$}			

TABLE IV: Eigenvalues E_{00} for $V(r) = -a/r + br^2$, $r \in (0, R)$, where we fixed $b = 0.5$ and we allowed a and R to vary. The subscript N refers to the number of iteration used by AIM.

$b = 0.5$								
a	R	E_{00}				R	a	E_{00}
1	0.1	468.994 438 340 395 273 843 _{$N=26$}				1	-10	24.446 394 090 129 924 468 _{$N=25$}
	0.5	14.781 525 455 450 240 772 _{$N=19$}					-5	15.581 919 590 917 726 881 _{$N=25$}
	1	2.500 000 000 000 000 000 _{$N=3, Exact$}					-1	7.427 602 986 235 605 737 _{$N=26$}
	2	0.281 457 639 408 567 801 _{$N=44$}					0	5.075 582 015 226 783 066 _{$N=26$}
	3	0.180 768 103 642 728 017 _{$N=66$}					1	2.500 000 000 000 000 000 _{$N=3, Exact$}
	4	0.179 669 842 444 710 526 _{$N=80$}					5	- 12.356 931 301 584 560 963 _{$N=35$}
	5	0.179 668 484 856 687 713 _{$N=82$}					10	- 49.984 937 021 677 890 425 _{$N=43$}

TABLE V: Eigenvalues E_{00} for $V(r) = -a/r + br^2$, $r \in (0, R)$, where we fixed $a = R = 1$ and allowed b to vary. The subscript N refer to the number of iterations used by AIM.

$R = 1, a = 1$	
b	E_{00}
0.1	2.399 281 395 696 719 214 _{$N=22$}
0.2	2.424 527 479 482 894 839 _{$N=22$}
0.5	2.500 000 000 000 000 000 _{$N=3$}
1.0	2.624 907 458 899 526 414 _{$N=31$}
2.0	2.871 465 192 314 860 746 _{$N=35$}
5.0	3.585 958 081 033 459 432 _{$N=41$}
10.0	4.698 782 960 476 752 179 _{$N=47$}

VI. SPECTRAL CHARACTERISTICS

In this section we shall discuss the spectral characteristics associated with the crossings of the energy levels. We have employed the generalized pseudo-spectral (GPS) Legendre method with mapping, which is a fast algorithm that has been tested extensively and shown to yield the eigenvalues with an accuracy of twelve digits after the decimal. A more detailed account, with several applications of GPS, can be found in [30–35] and the references therein.

In the present work, we have also verified the accuracy of these results, in a few selected cases, by using AIM. We shall first consider the case defined by $R \rightarrow \infty, a = 1$ and variable b , under which the potential given by Eq.(1) can

be regarded as representing the hydrogen atom confined by a soft harmonic oscillator potential. Starting from the free HA ($b = 0$), the effect of finite b is to remove the accidental degeneracy and raise the energy levels such that $E(\nu, \ell) > E(\nu, \ell + 1)$ (see Ref. [36]). As the starting $E(\nu, \ell) < 0$ given by the HA spectrum, there exists a critical value of $b = b_c$, corresponding to each level, defined by the condition $E(\nu, \ell) = 0$. The numerical values of b_c are found to be rather small, except for the ground state, indicating that a weak confinement due to the harmonic potential is sufficient to realize the condition that $E(\nu, \ell) > 0$ for all $b > b_c$. In the usual spectroscopic notations the levels

$$(1s2s2p3s3p3d4s4p4d4f)$$

are defined by the b_c values given respectively by

$$b_c = (0.32533, 0.004831, 0.00771, 0.00042, 0.00051, 0.00079, 0.00007, 0.00008, 0.00010, 0.00015).$$

In Fig. 1, we have displayed the passing of the energy levels corresponding to $4s4p4d4f$ states through $E = 0$ at b_c . We know tht the eigenspectrum of free HA is indeed very sensitive to the harmonic confinement since it is found numerically that at $b = 0.000001$, the eigenvalues are already positive, corresponding to the states given by $7p, 7d, 8d, \dots, 7f, 8f, \dots, 7g, \dots$. The crossings of energy levels can be gauged by the change of ordering from the hydrogen-like

$$(1s2p2s3d3p3s4f4d5g4p4s5f5d6g5p5s6f6d7g6p6s7f7d8g7p8f8d9g9f \dots)$$

to

$$\rightarrow (1s2p2s3d3p4f3s4d5g4p5f4s5d6g5p6f5s6d7g6p7f6s7d8g7p8f8d9g9f \dots)$$

as the parameters of the potential change along $(a = 1, b = 0) \rightarrow (a = 1, b = 0.001) \rightarrow (a = 1, b = 0.5)$. It follows that the $(3s, 4f), (4s, 5f) \dots$ levels defined by (ν, ℓ) and $(\nu + 1, \ell + 3)$ cross at a certain b .

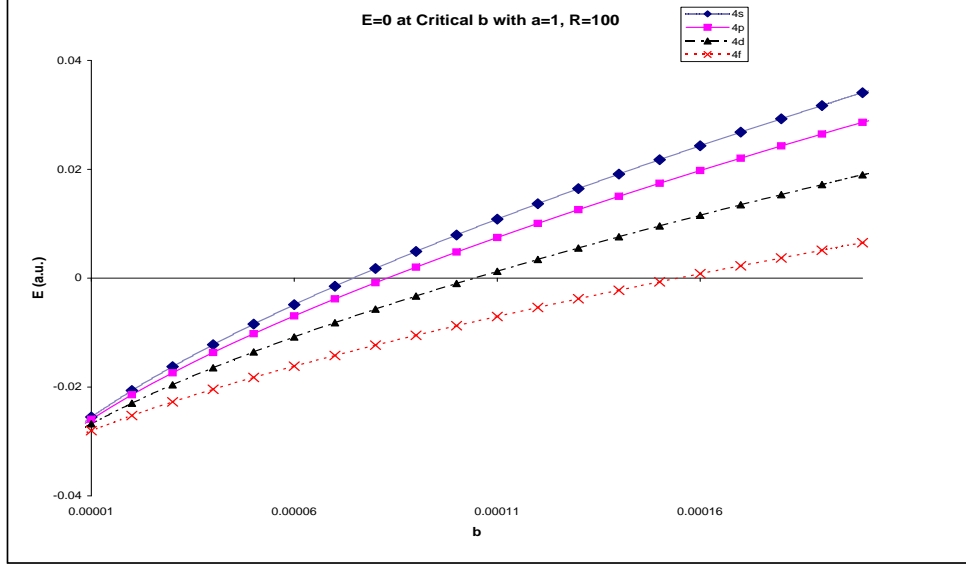


FIG. 1: The critical b , denoted as b_c in the text at which $E(\nu, \ell) = 0$ are shown for the $4s, 4p, 4d, 4f$ states. The large value of $R = 100$ corresponds essentially to the free state of the potential in Eq.(1) with $a = 1$.

In Fig. 2, we have displayed this behavior corresponding to $a = 1$. This spectral characteristic is similar to that found earlier [37] for the case of the soft Coulomb potential. Further, the eigenvalue $(\nu = 5, \ell = 4)$ is found to cross $(\nu - 1, \ell - 4), (\nu - 1, \ell - 3)(\nu, \ell - 4), (\nu, \ell - 3)(\nu, \ell - 2), (\nu, \ell - 1)$ as b changes from 0 to 0.5.

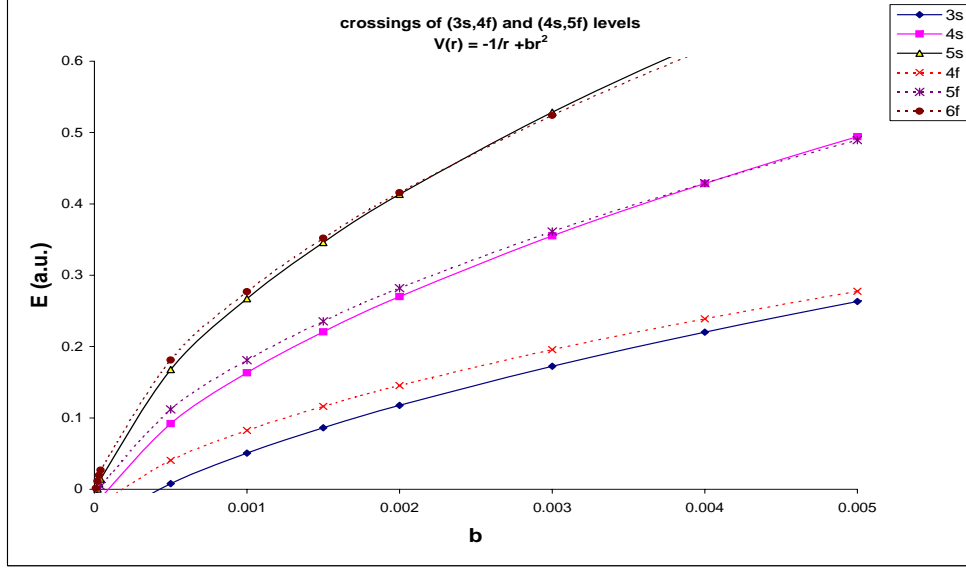


FIG. 2: The crossings of levels as a function of b , corresponding to the free state of the potential in Eq.(1) with $a = 1$. The levels defined by (ν, ℓ) and $(\nu + 1, \ell + 3)$ are shown.

Next, we consider the new spectral characteristics introduced when, in addition to the harmonic-oscillator potential term, a second confining feature consisting of an impenetrable sphere of finite radius R is introduced. Such a potential factor further raises the energy levels as R is diminished, $\rightarrow 0$. As a consequence the b_c values get smaller. This is depicted in Fig. 3 for the $4s$ and $4p$ states at two different values of R of 100 and 30 a.u., respectively. The former corresponds to the case $R \rightarrow \infty$, i.e. just the potential in Eq.(1). Varying R under fixed a yields a different level ordering, depending upon the value of b , as this situation corresponds to two specifically chosen confinement features imposed on the hydrogen-like potential at each point. To illustrate this, we consider the case defined by $a = 1$, $b = 0.5$ and variable R . Our calculations suggest that the ordering of levels changes from

$$(1s2p2s3d3p4f3s4d5g4p5f4s5d6g5p6f5s6d7g6p7f6s7d8g7p8f8d9g9f10g\dots)$$

to

$$\rightarrow (1s2p3d2s4f3p5g4d3s5f4p6g5d4s6f5p7g6d5s7f6p8g7d6s8f7p9g8d9f10g\dots)$$

as R changes from $\infty \rightarrow 0$. The crossings of levels are now observed between the state (ν, ℓ) and $(\nu - 1, \ell + 2)$. In Fig. 4, we have shown this feature corresponding to the confined $(3s, 4d)$ and $(3s, 4f)$ states. Additionally, the $5g$ level is found to fall below $4d$ and $3s$ levels, successively, as R decreases. It is evident that the imposition of a double confinement effect, mediated through the combination of br^2 and the boundary at R leads to the crossings among a wider set of the states of the hydrogen-like atom, not observed in the separate singly confined situations. A possible experimental system of embedded atom inside zeolite, fullerene, or liquid helium droplets under very strong laser fields could be modelled using the doubly confined Coulomb potential as described in this work.

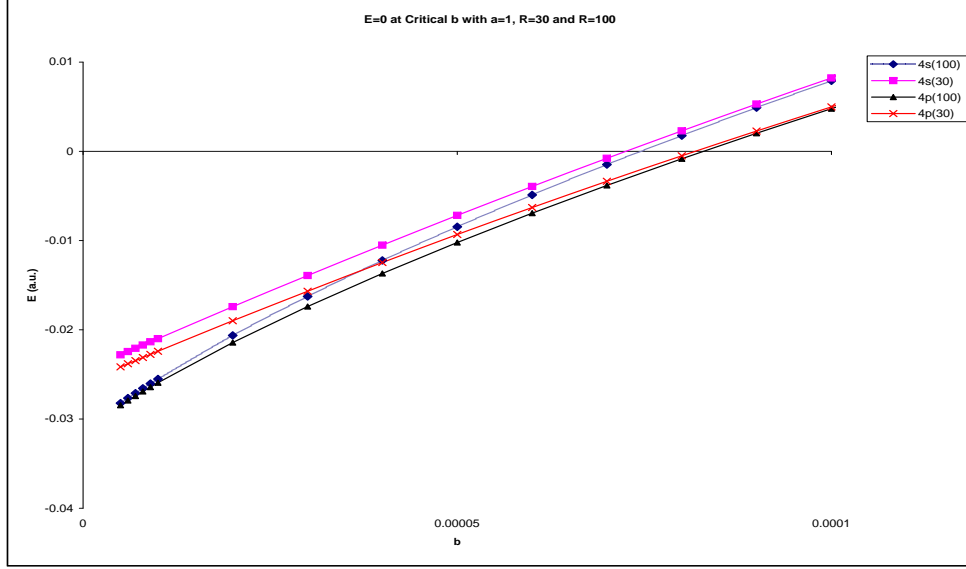


FIG. 3: The critical b , denoted as b_c in the text at which $E(\nu, \ell) = 0$ are shown for the $4s, 4p$ states. The value of b_c decreases as R decreases: specifically, the essentially free state of the potential in Eq.(1) with $a = 1$ at $R = 100$ is confined to a smaller value of $R = 30$. The numbers inside brackets denote R .

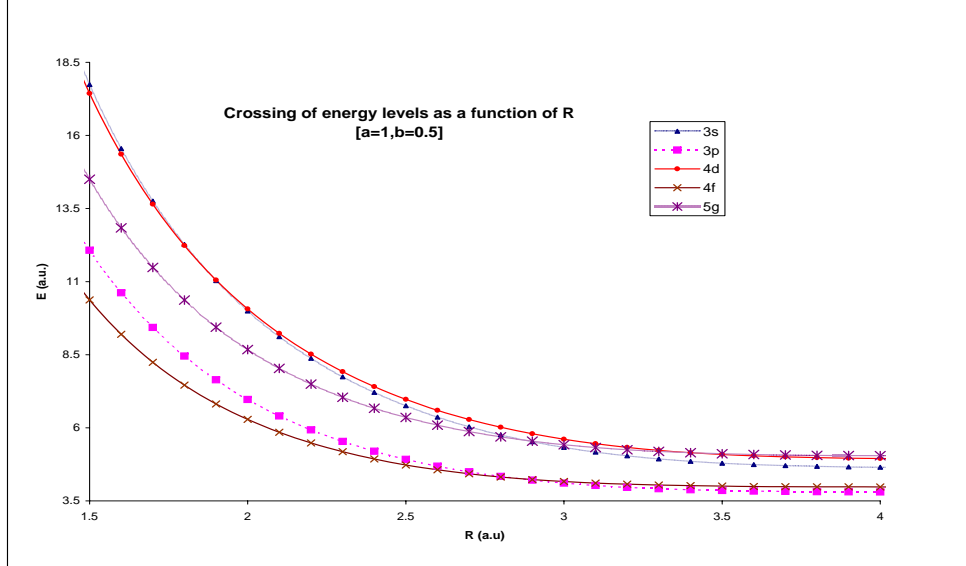


FIG. 4: The crossings of levels as R is changed as the potential in Eq.(1) is defined by the values $a = 1$ $b = 0.5$. Crossings are observed between the state (ν, ℓ) and $(\nu - 1, \ell + 2)$ as shown by the $(3s, 4d)$ and $(3s, 4f)$ levels. The $5g$ level is shown to cross $4d$ and $3s$ as R decreases.

VII. CONCLUSION

In this study we first consider a very elementary model for an atom, namely a single particle which moves in a central Coulomb potential $-a/r$ and obeys quantum mechanics. We then adjoin two confining features: soft confinement by means of an attractive oscillator term br^2 , and hard confinement produced by containment inside an impenetrable spherical cavity of radius R . The paper reports on the effects of the confinement parameters $\{b, R\}$ on the original Coulomb spectrum which, of course, is given in atomic units by $E = -a^2/(2\nu^2)$. By a combination of analytical and numerical techniques, we are able to make considerable progress in analyzing the spectral characteristics of this confined atomic model. In future work we plan to undertake a similar study in which the pure Coulomb term is replaced by a more physically interesting screened-Coulomb potential, or a soft-core potential such as $-a/(r + \beta)$. The purpose of this work is to look at model problems that contain physically interesting features but are still simple enough to yield to analytical as well as purely numerical analysis.

VIII. ACKNOWLEDGMENTS

Partial financial support of this work under Grant Nos. GP3438 and GP249507 from the Natural Sciences and Engineering Research Council of Canada is gratefully acknowledged by two of us (RLH and NS). KDS is grateful to the Shastri Indo-Canadian Institute, Calgary, for a partial travel grant. NS and KDS are also grateful for the hospitality provided by the Department of Mathematics and Statistics of Concordia University, where part of this work was carried out.

-
- [1] A. Michels, J. de Boer, and A. Bijl, *Physica* **4**, 981 (1937).
 - [2] A. Sommerfeld and H. Welker, *Ann. Physik* **32**, 56 (1938).
 - [3] B.L. Burrows and M. Cohen, *Phys. Rev. A* **72**, 032508 (2005).
 - [4] J.C. Stewart and K.D. Pyatt, *Phys. Rev.* **144**, 1203 (1966).
 - [5] S. Skupsky, *Phys. Rev. A* **21**, 1316 (1980).
 - [6] R. Cauble, M. Blaha, and J. Davis, *Phys. Rev. A* **29**, 3280 (1984).
 - [7] S.A. Cruz (Guest Editor) *Adv. Quant. Chem.* **57**, 1-334 (2009); *ibid* **58**, 1-279 (2009).
 - [8] I.G. Ryabinkin and V.N. Staroverov, *Phys. Rev. A* (In Press).
 - [9] A. V. Scherbinin, V. I. Pupyshev and A. Yu. Ermilov *Physics of Clusters* p. 273 (Singapore: World Scientific, 1997).
 - [10] K.D. Sen, H.E. Montgomery, Jr. and N.A. Aquino, *Intl. J. Quantum Chem.* **107**, 798 (2007).
 - [11] F.M. Fernandez, A.M. Meson and E.A. Castro, *Phys. Lett. A* **111**, 104 (1985).
 - [12] E. Castro and P. Martin, *J. Phys. A: Math. Gen.* **33**, 5321 (2000).
 - [13] M. Alberg and L. Wilets, *Phys. Lett. A* **286**, 7 (2001).
 - [14] S.H. Patil and Y.P. Varshni, *Can. J. Phys.* **82**, 917 (2004).
 - [15] K.D. Sen, V. I. Pupyshev and H.E. Montgomery Jr., *Ad. Quantum Chem.* **57**, 25 (2009).
 - [16] M. Reed and B. Simon, *Methods of modern mathematical physics II: Fourier analysis and self-adjointness*, (Academic Press, New York, 1975). [The operator inequality is proved on p 169].
 - [17] S. J. Gustafson and I. M. Sigal, *Mathematical concepts of quantum mechanics*, (Springer, New York, 2006). [The operator inequality is proved for dimensions $d \geq 3$ on page 32.]
 - [18] A. K. Common, *J. Phys. A* **18**, 2219 (1985).
 - [19] R. L. Hall, *Phys. Rev. D* **22**, 2062 (1980).
 - [20] R. L. Hall, *J. Math. Phys.* **24**, 324 (1983).
 - [21] R. L. Hall, *J. Math. Phys.* **25**, 2708 (1984).
 - [22] R. L. Hall, *Phys. Rev. A* **39**, 550 (1989).
 - [23] R. L. Hall, *J. Math. Phys.* **33**, 1710 (1992).
 - [24] R. L. Hall, *J. Math. Phys.* **34**, 2779 (1993).
 - [25] H. Ciftci, R. L. Hall, and Q. D. Katatbeh, *J. Phys. A* **36**, 7001 (2003).
 - [26] H. Ciftci, R. L. Hall, N. Saad, and E. Dogu, *J. Phys. A: Math. Theor.* **43**, 415206 (2010).
 - [27] Richard L. Hall, Nasser Saad, K. D. Sen and Hakan Ciftci, *Energies and wave functions for a soft-core Coulomb potential*, *Phys. Rev. A* **80** (2009) 032507.
 - [28] Hakan Ciftci, Richard L. Hall, and Nasser Saad, *Asymptotic iteration method for eigenvalue problems*, *J. Phys. A* **36** (2003) 11807-11816.
 - [29] Champion Brodie, Richard L. Hall, Nasser Saad, *Asymptotic Iteration Method for Singular Potentials*, *Int. J. Mod. Phys. A* **23** (2008) 1405.
 - [30] G. Yao and S. I. Chu, *Chem. Phys. Lett.* **204**, 381 (1993).
 - [31] J. Wong, S. I. Chu and C. Laughlin, *Phys. Rev. A* **50**, 3208 (1994).
 - [32] X. M. Tong and S. I. Chu, *Phys. Rev. A* **64**, 013417 (2001).
 - [33] A. K. Roy and S. I. Chu, *Phys. Rev. A* **65**, 043402 (2002). *ibid.* **65**, 052508 (2002).
 - [34] K.D. Sen and A.K. Roy, *Phys. Lett. A.* **357**, 112 (2006).
 - [35] H.E. Montgomery Jr., N.A. Aquino and K.D. Sen, *Int. J. Quantum Chem.* **107**, 798 (2007).
 - [36] B. Baumgartner, H. Grosse, and A. Martin, *Phys. Lett. B* **146**, 363 (1984).
 - [37] R. L. Hall, N. Saad, K.D. Sen, and H. Ciftci, *Phys. Rev. A* **80**, 03250 (2009).